This is the peer-reviewed, final accepted version for American Mineralogist, published by the Mineralogical Society of America.
The published version is subject to change. Cite as Authors (Year) Title. American Mineralogist, in press.
DOI: https://doi.org/10.2138/am-2022-8365. http://www.minsocam.org/

Revision 1

Finchite, $Sr(UO_2)_2(V_2O_8)\cdot 5H_2O$, a new uranyl sorovanadate with the francevillite anion topology

Tyler L. Spano[1,2§], Travis A. Olds[1,3], Susan M. Hall[4], Bradley S. Van Gosen[4], Anthony R. Kampf[5], Peter C. Burns[1,6], Joe Marty[7]

[1] Department of Civil and Environmental Engineering and Earth Sciences, University of Notre Dame, Notre Dame, IN 46556, USA

[2] Nuclear Nonproliferation Division, Oak Ridge National Laboratory, Oak Ridge, TN 37830, USA

[3] Section of Minerals and Earth Sciences, Carnegie Museum of Natural History, 4400 Forbes Avenue, Pittsburgh, PA 15213, USA

[4] U.S. Geological Survey, Box 25046, MS 939, Denver, CO 80225

[5] Mineral Sciences Department, Natural History Museum of Los Angeles County, 900 Exposition Boulevard, Los Angeles, CA 90007, USA

[6] Department of Chemistry and Biochemistry, University of Notre Dame, Notre Dame, IN 46556, USA

[7] 5199 East Silver Oak Road, Salt Lake City, UT 84108, USA

ABSTRACT

Finchite (IMA2017-052), $Sr(UO_2)_2(V_2O_8)\cdot 5H_2O$, is the first uranium mineral known to contain essential Sr. The new mineral occurs as yellow-green blades up to ~10 μm in length in surface outcrops of the calcrete-type uranium deposit at Sulfur Springs Draw, Martin County, Texas, USA. Crystals of finchite were subsequently discovered underground in the Pandora mine, La Sal, San Juan County, Utah, USA, as diamond-shaped golden-yellow crystals reaching up to 1 mm. The crystal structure of finchite from both localities was determined using single crystal X-ray diffraction and is orthorhombic, *Pcan,* with a = 10.363(6) Å, b = 8.498(5) Å, c = 16.250(9) Å, V = 1431.0(13) Å^3, Z = 4 (R_1 = 0.0555) from Sulfur Springs Draw; and a =

§ Email: spanotl@ornl.gov

10.3898(16), b = 8.5326(14), c = 16.3765(3) Å, V = 1451.8(4) Å^3, Z = 4 (R_1 = 0.0600) from the Pandora mine. Electron-probe microanalysis provided the empirical formula $(Sr_{0.88}K_{0.17}Ca_{0.10}Mg_{0.07}Al_{0.03}Fe_{0.02})\Sigma_{1.20}(UO_2)_2(V_{2.08}O_8)\cdot 5H_2O$ for crystals from Sulfur Springs Draw, and $(Sr_{0.50}Ca_{0.28}Ba_{0.22}K_{0.05})_{\sum 0.94}(U_{0.99}O_2)_2(V_{2.01}O_8)\cdot 5H_2O$ for crystals from the Pandora mine, based on 17 O atoms per formula unit. The structure of finchite contains uranyl vanadate sheets based upon the francevillite topology. Finchite is a possible immobilization species for both uranium and the dangerous radionuclide ^{90}Sr because of the relative insolubility of uranyl vanadate minerals in water.

INTRODUCTION

Uranyl vanadate minerals are ubiquitous where uranium and vanadium ore has oxidized due to their limited aqueous solubility over a range of geochemical conditions (Barton 1958; Weeks 1961; Tokunaga 2012; Plášil 2014) and are important in limiting the environmental mobility of the UO_2^{2+} uranyl ion (Avasarala et al. 2017). Several uranyl vanadate minerals contain sheets with the francevillite anion topology, which is compatible with interstitial cations of varying size, coordination, and ionic charge (Cesbron and Morin 1968; Krivovichev et al. 2013), leading to extensive solid solution between species (Spano et al. 2017a). Finchite, a newly recognized uranyl vanadate mineral species described herein, possesses the francevillite anion topology and represents a Sr-bearing end-member of the francevillite–curienite solid solution series (Spano et al. 2017b).

The name *finchite* honors American uranium geologist Warren I. Finch (1924–2014). Mr. Finch worked at the U.S. Geological Survey (USGS) as a uranium resource specialist for 50 years, and the new mineral was discovered as part of a continuation of the exploration program that he devoted his life to promoting. Mr. Finch received his bachelor's of science

degree in geological engineering from the South Dakota School of Mines and Geology in 1948 and his master's of science degree in geology from the University of California, Berkeley, in 1954. He pursued additional graduate study at the Colorado School of Mines from 1958 to 1959. Mr. Finch first joined the USGS in 1948 as a field assistant and spent his entire 50-year professional career at that institution, advancing to the rank of senior scientist. He was awarded the Meritorious (1981) and Distinguished (1994) Service Awards from the Department of the Interior and served as the first chief of the Uranium and Thorium Resources Branch from 1973 to 1979. In 1974, he began a decades-long association with the International Atomic Energy Agency, serving as U.S. representative and technical expert in the areas of uranium resources, uranium resource estimation, and particularly the geology of sandstone-hosted uranium deposits. In this capacity, Mr. Finch was privileged to visit many of the major uranium deposits of the world. Mr. Finch published extensively, including the highly cited 1967 USGS professional paper "Geology of epigenetic uranium deposits in sandstone in the United States," which is still recognized as a definitive work on the subject (Finch 1967). This publication was the culmination of many years (1949–1961) devoted to his career-long fascination with the uranium geology and uranium resources of the Colorado Plateau region, which continue to be explored today.

Samples of finchite are deposited in the mineralogical collections of the Natural History Museum of Los Angeles County, 900 Exposition Boulevard, Los Angeles, CA 90007, USA, catalogue numbers 66476 and 66477.

OCCURRENCE

Finchite was found in surface outcrops approximately 21 miles south–southeast of Lamesa, Texas, on the eastern edge of Sulfur Springs Draw, Martin County, Texas. A calcrete-

type uranium deposit, the Sulfur Springs Draw Deposit, was identified in this area by the Kerr-McGee Corporation in the late 1970s by aerial radiometric surveys of the region (Van Gosen and Hall 2017; Hall et al. 2019). Uranium mineralization is concentrated just above the modern water table in a 30-meter-thick section of calcareous siltstones and fine-grained sandstones capped by pedogenic calcrete up to 6 meters thick. The deposit is partially exposed along the edge of Sulfur Springs Draw by a farm road that was cut into caprock to access the draw. USGS geologists located the exposed mineralization in 2015 and collected samples of yellow uranyl vanadates that coat grains, fill vugs, and line fractures in a calcareous, very fine-grained to fine-grained sandstone and massive carbonate (Figure 1).

Figure 1. Finchite and carnotite coating dolomite, Sulfur Springs Draw, Texas.

Finchite is found in the late Pleistocene Tahoka Formation (Hall et al. 2019), which is thought to be lacustrine based on regional facies relationships and fossil evidence (Frye 1968; Van Gosen and Hall 2017). The Tahoka Formation is exposed rimming approximately 30 large

saline lakes of the Southern High Plains. It is a fine-grained, locally calcareous and gypsiferous sandstone that grades laterally into gravel deposits. In the exploration model employed by Kerr-McGee, the lacustrine strata that host the Sulphur Springs Draw and nearby Buzzard Draw deposits were genetically associated with a large Pleistocene lake located downstream. This large prehistoric saline lake has been named Lake Lomax and is the largest Pleistocene-age lake identified in the Southern High Plains region (Frye 1968; Van Gosen and Hall 2017).

At Sulfur Springs Draw, finchite occurs intimately with carnotite and appears as disseminated pore fill and as cross-cutting veinlets in the micritic dolomite host (Figure 2). Paragenetically later than carnotite, finchite occurs predominantly as bladed crystals and crystal aggregates up to approximately 10 μm in width, and as late-stage space fill of powdery masses (Figure 2a–c). Crystals exceeding 10 μm are rare, which is likely due to the low solubility of finchite, causing it to precipitate in very fine-grained crystals. In places, finchite coats earlier carnotite and (Figure 2c) and is intergrown with celestine (Figure 2b), the later indicating that the fluids that formed finchite had become rich in Sr. Finchite likely formed under evaporative conditions from fluids at approximately ambient surface temperatures (Ranalli and Yager 2016), which is supported by the presence of accompanying dolomite and celestine. Other associated minerals include quartz, illite, and an unidentified amorphous Sr-rich carbonate species.

This is the peer-reviewed, final accepted version for American Mineralogist, published by the Mineralogical Society of America.
The published version is subject to change. Cite as Authors (Year) Title. American Mineralogist, in press.
DOI: https://doi.org/10.2138/am-2022-8365. http://www.minsocam.org/

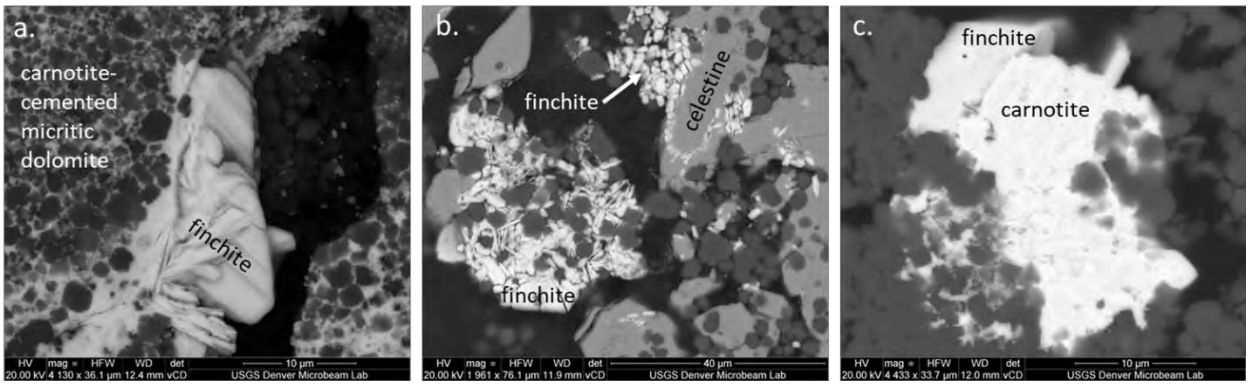

Figure 2. a. Backscatter SEM image of finchite crystals (Sulfur Springs Draw) filling a vug within micritic carnotite-cemented dolomite. b. Finchite intergrown with celestine in micritic dolomite. C. Finchite associated with carnotite.

Crystals of finchite were subsequently discovered underground in the Pandora mine, La Sal, San Juan County, Utah, where it occurs as coatings on pandoraite-Ca and pandoraite-Ba, on sandstone (Figure 3). The Pandora mine is located within the Paradox Valley district which was formed by uplift and erosion of a salt anticline resulting in exposure of ore-bearing sandstone (Carter and Gualtieri 1965). Significant bleaching alteration has been observed in this area evidenced by gas fields in the Paradox Valley region, and petrographically through hematite crystals preserved by quartz overgrowth. Bleaching alteration is intimately associated with uranium and vanadium deposits here and has been proposed to either reduce hematite to pyrite or reduce hematite and lead to dissolved Fe^{2+} and subsequent mobility away from host rocks. Regardless of the mode of bleaching, the presence of hydrocarbons is believed to be the mechanism responsible for alteration (Barton et al. 2018). Uranium and vanadium mineralization at the Pandora mine was deposited under reducing conditions as solutions containing these elements contacted accumulations of carbonaceous material, depositing uraninite and montroseite- corvusite ore (Kampf et al. 2019). Post mining oxidation of these montroseite-corvusite ores led to crystallization of finchite. At the Pandora mine, finchite specimens occurs as aggregates and individuals reaching up to 100 μm in width (Figure 3).

This is the peer-reviewed, final accepted version for American Mineralogist, published by the Mineralogical Society of America.
The published version is subject to change. Cite as Authors (Year) Title. American Mineralogist, in press.
DOI: https://doi.org/10.2138/am-2022-8365. http://www.minsocam.org/

Figure 3. Finchite and pandoraite-Ca from the Pandora Mine, La Sal Mining District, San Juan County, Utah. Horizontal field of view is 1.13 mm.

PHYSICAL AND OPTICAL PROPERTIES

Finchite crystals from both localities are bright yellow with a light-yellow streak and a pearly, transparent luster. Based on scratch tests, the Mohs hardness of finchite is approximately 2, and crystals are characterized by brittle tenacity, irregular fracture, perfect cleavage on (001) (Figure 4), and parting was not observed. Finchite does not fluoresce under short or long wave ultraviolet light. Optically, finchite from the Pandora mine is biaxial (–), with $\alpha = 1.70(1)$, $\beta = 1.85(1)$, and $\gamma = 1.90(1)$ (measured in white light). The $2V$ measured directly on a spindle stage is 53(1)°; the calculated $2V$ is 55.9°. Dispersion is $r < v$, slight. The mineral is pleochroic: X = colorless, Y and Z are yellow; $X < Y \approx Z$. The optical orientation is X = **c**, Y = **a**, and Z = **b**. Note that the murkiness of the crystals required them to be split into thin cleavage fragments for the index of refraction measurements, which made the measurement of α particularly difficult because it is oriented perpendicular to the cleavage.

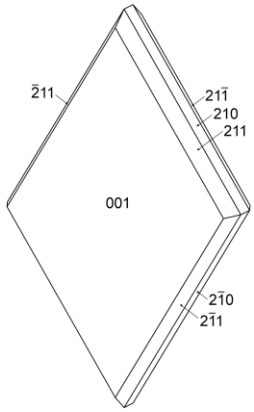

Figure 4. Crystal drawing of finchite from the Pandora mine; clinographic projection in nonstandard orientation, [100] vertical.

The calculated density of finchite is 4.429 and 4.352 g*cm^{-3} based on the empirical and ideal formulae, respectively. The density could not be measured directly because it is higher than that of Clerici solution. The predicted average index of refraction based upon the Gladstone–Dale relationship is 1.85, using k(UO_3) = 0.134 under the assumption that vanadates are analogous to uranyl phosphates and arsenates (Piret and Deliens 1989).

INFRARED SPECTROSCOPY

Attenuated total reflectance Fourier transform infrared spectra were obtained using a liquid N_2-cooled SENSIR Technologies IlluminatIR mounted to an Olympus BX51 microscope. An attenuated total reflectance objective was pressed into crystals of finchite and the spectrum was measured from 4000 to 650 cm^{-1} (Figure 5). The ν OH stretching vibrations of interstitial H_2O groups occur between ~2800 and 3600 cm^{-1}, with a maximum intensity occurring at 3282 cm^{-1}. Approximate O–H···O hydrogen bond lengths calculated from the observed stretching frequencies lie within the range 2.9 to 2.6 Å using the correlation function given by Libowitzky (1999). The medium strong band at 1615 cm^{-1} is assigned as the ν_2 (δ)-bending vibrations of interstitial water molecules. The band located at 1415 cm^{-1} may be a combination band but likely

169 corresponds to the asymmetric stretching of ν_3 CO_3, originating from the close association of
170 finchite with dolomite (Gunasekaran et al. 2006).

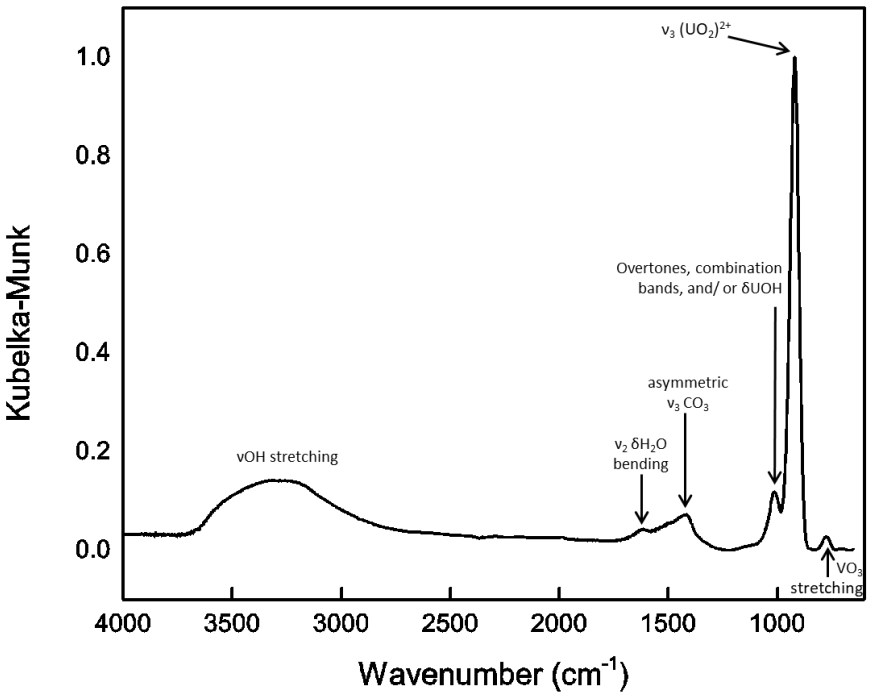

171

172 *Figure 5. The infrared spectrum (attenuated total reflectance) of finchite.*

173 The strong antisymmetric uranyl stretch, ν_3 $(UO_2)^{2+}$, occurs at 920 cm^{-1}, and VO_3
174 stretching modes are visible at 773 cm^{-1} (Cejka 1999). The uranyl cation bond length inferred
175 from the 920 cm^{-1} mode of finchite using the empirical relations given by Jones (1958) and
176 Glebov (1982) is 1.79 Å, which is in excellent agreement with our X-ray crystallographic results.
177 No evidence is found for the presence of the IR-forbidden symmetric ν_1 $(UO_2)^{2+}$ stretch.
178 However, a weak band at 1011 cm^{-1} may be attributed to δ-U–O modes of equatorial O atoms, or
179 to combination bands or overtones (Cejka 1999).

This is the peer-reviewed, final accepted version for American Mineralogist, published by the Mineralogical Society of America.
The published version is subject to change. Cite as Authors (Year) Title. American Mineralogist, in press.
DOI: https://doi.org/10.2138/am-2022-8365. http://www.minsocam.org/

CHEMICAL ANALYSIS

Chemical analyses on crystals from both localities were performed using a JEOL JXA-8900 electron microprobe operating at an accelerating voltage of 15 kV, with a beam current of 20 nA and 1 μm spot diameter. Matrix effects were accounted for using the $\phi(\rho z)$ correction routine (Armstrong 1988). The empirical formula is calculated on the basis of 17 O and 2 U *apfu*. Finchite from the Sulfur Springs Draw Deposit contains appreciable U, V, and Sr, with Ca and minor Mg, Fe, Al, and K, with analytical results listed in Table 1. Owing to the small crystal size and intimate association of finchite with carnotite and dolomite, the measured Ca concentrations are likely higher than the actual content of finchite. Furthermore, significant dehydration occurred upon contact of finchite with the microprobe beam leading to anomalously high totals for all elements. Normalized data are also provided in Table 1. Because of the limited amount of material available, the H_2O content was not measured and is instead calculated by stoichiometry with respect to the structure, which on the basis of 17 O *apfu*, provided the empirical formula $(Sr_{0.88}K_{0.17}Ca_{0.10}Mg_{0.07}Al_{0.03}Fe_{0.02})\Sigma_{1.20}(UO_2)_2(V_{2.08}O_8)\cdot 5H_2O$. The normalized values are in good agreement with the ideal formula $Sr(UO_2)_2(V_2O_8)\cdot 5H_2O$ calculated from X-ray crystallographic results, which requires SrO 10.96, UO_3 60.35, V_2O_5 19.19, and H_2O 9.50, totaling 100 wt%.

Crystals of finchite from the Pandora mine, which were much larger, presented less difficulties during chemical analysis. The empirical formula (calculated on the basis of 17 O *apfu*) is $(Sr_{0.50}Ca_{0.28}Ba_{0.22}K_{0.05})\Sigma_{0.94}(U_{0.99}O_2)_2(V_{2.01}O_8)\cdot 5H_2O$.

X-RAY CRYSTALLOGRAPHY AND STRUCTURE DETERMINATION

Single-crystal X-ray diffraction data were collected for finchite from Sulfur Springs Draw using a Bruker Apex II CCD-based detector mounted on a three-circle Bruker Apex II Quazar diffractometer with a microfocus source utilizing monochromated Mo*K*α radiation (λ =

This is the peer-reviewed, final accepted version for American Mineralogist, published by the Mineralogical Society of America.
The published version is subject to change. Cite as Authors (Year) Title. American Mineralogist, in press.
DOI: https://doi.org/10.2138/am-2022-8365. http://www.minsocam.org/

0.709 Å). Reflections were integrated and corrected for Lorentz, polarization, and background effects using the Bruker program SAINT. A multiscan semiempirical absorption correction was applied using equivalent reflections in SADABS-2012 (Bruker 2009). An initial structure model was obtained by the intrinsic phasing method using SHELXT (Sheldrick 2015a) in the space group *Pcan*. Refinement proceeded by full-matrix least-squares on F^2 using SHELXL-2016 (Sheldrick 2015b). Additional refinement details for Sulfur Springs Draw and Pandora Mine samples are included in Table 2.

DESCRIPTION OF THE STRUCTURE

The structure solution of finchite from both localities located one U, one V, and six O sites that make up a uranyl vanadate sheet, as well as one interstitial cation site occupied predominantly by Sr (Figure 6). Chemical analyses indicate finchite from Sulfur Springs Draw contains appreciable Ca and K at this site as well, and that finchite from the Pandora mine contains significant Ca and Ba substitution. Three O atoms belonging to H_2O groups were also located between the uranyl vanadate sheets. Positional and anisotropic displacement parameters were successfully refined for all non-H atoms; however, a subsequent difference-Fourier synthesis did not provide plausible H atom sites. Atomic coordinates and displacement parameters for each refinement are contained in Supporting Information Tables S1 and S2, with selected bond distances in Tables S3 and S4, and results of bond valence analyses in Tables S5 and S6 for Sulfur Springs and Pandora finchite samples, respectively.

During refinement of finchite from Sulfur Springs draw, an initial model was produced using free refinement of the interstitial cation site occupancy as only Sr. This resulted in an occupancy of 1.05 Sr, suggesting that a heavier element may be present, or indicating a non-ideal absorption correction. Instead, we forced the interstitial cation occupancies to match those

This is the peer-reviewed, final accepted version for American Mineralogist, published by the Mineralogical Society of America.
The published version is subject to change. Cite as Authors (Year) Title. American Mineralogist, in press.
DOI: https://doi.org/10.2138/am-2022-8365. http://www.minsocam.org/

measured by electron microprobe. When modeled this way, the structure remains nearly identical to our initial solution, yielding only a slight improvement in the agreement index.

During the refinement of the Pandora mine finchite structure, attempts to model the interstitial site as (Sr, Ca, Ba) = 1, yielded a site containing very little Ca, ~0.8 Sr, and ~0.2 Ba. Resultingly, we forced the site composition and occupancy to match that determined by EMPA ($Sr_{0.5}$, $Ca_{0.28}$, and $Ba_{0.22}$) giving an agreement index of R1 = 0.06, wR2 = 0.17, slightly worse than our refinement with only Sr and Ba present. This could indicate that the crystal used for structure determination possesses slightly higher Sr and Ba content, and no Ca relative to the crystal examined with EMPA. However, it is likely that substitution introduces positional disorder, given the large differences in the ionic radii and bonding requirements of Ca, Sr, and Ba, such that these atoms do not sit precisely at the site defined by the EAXY, EADP position and ellipsoid.

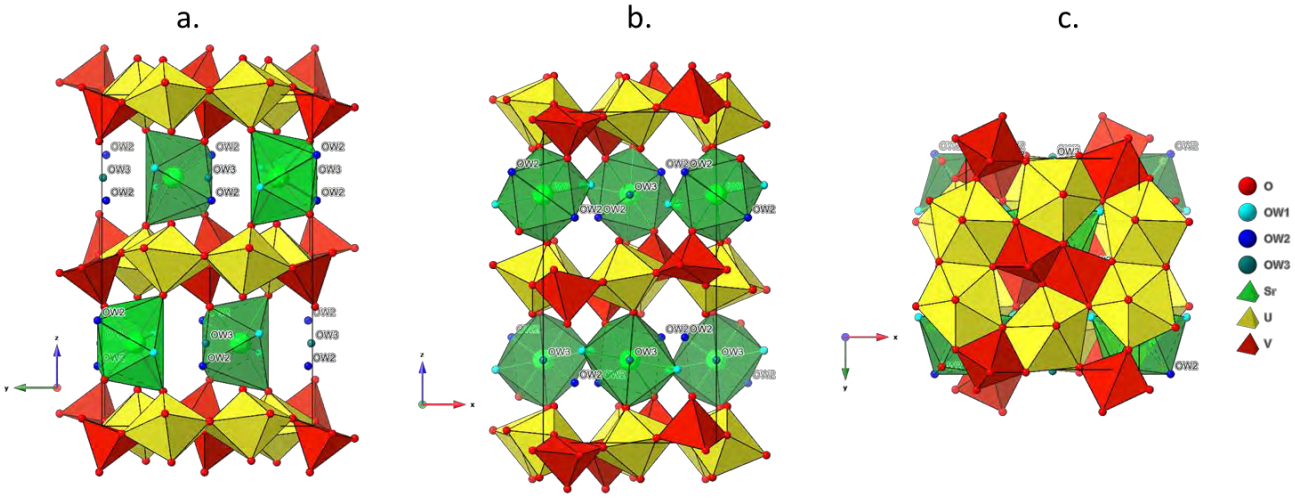

Figure 6. The crystal structure of finchite.

As in other uranyl vanadate minerals and synthetic U(VI) vanadate compounds, U atoms are strongly bonded to two O, giving the approximately linear uranyl ion UO_2^{2+} (Burns et al.

1997). Further coordination by five O in the equatorial plane, perpendicular to axial uranyl O atoms, results in pentagonal bipyramidal coordination geometries. Pairs of pentagonal bipyramidal U polyhedra share an edge, forming dimers. Similarly, V in the anionic sheet occupies V_2O_8 dimers, where each V atom forms slightly distorted edge-sharing square pyramidal polyhedra with the apex of each pyramid pointing in opposite directions. Pairs of uranyl pentagonal bipyramids and V_2O_8 dimers form sheets that extend along [100] and [010] (Figure 6), an identical structural unit found in other uranyl sorovanadates (Krivovichev et al. 2013; Spano et al. 2017b). In particular, the U & V sheet in finchite is indistinguishable from those of francevillite and curienite (Cesbron and Morin 1968), as well as metatyuyamunite (Burciaga-Valencia 2010). Additionally, chemical analyses indicate that finchite contains K, Ca, Mg, Al, and Fe substituting for Sr. This is unsurprising given the extensive solid solution present in the francevillite–curienite series and the close association of carnotite, tyuyamunite, and strelkinite (K, Ca, and Al uranyl vanadates), respectively, in most U–V-bearing deposits (Finch 1967).

The uranyl vanadate sheets in finchite are linked through interstitial Sr^{2+} in eightfold coordination as well as by an extensive network of H bonds formed between interstitial water and O atoms of the sheet (Figure 6a–c). Sheets are stacked parallel to [001], corresponding to the observed plane of perfect cleavage (Figure 6c). Four O atoms that coordinate Sr belong to the $[(UO_2)_2(V_2O_8)]^{2-}$ sheets on either side (Figure 6a–b). Two O atoms coordinating Sr are apical O atoms of V_2O_8 units (O6), and an additional two O atoms coordinating Sr are those of the uranyl O atom O4 (Figure 6a–b). The remaining four O bonded to Sr belong to water (O_{w1} and O_{w2}) (Figure 6a–b). O_{w1} and O_{w2} likely participate in H bonding among themselves and to interstitial

264 O_{w3}, which is held in place by H bonding only, and the O_{yl} atom O2 located within the
265 $[(UO_2)_2(V_2O_8)]^{2-}$ sheet (Figure 6a–b).

266 Material paucity and the intimate association with carnotite, dolomite, and celestine
267 (Figure 2) precluded collection of powder X-ray diffraction data of finchite from Sulfur Springs
268 Draw, Texas. However, powder diffraction data were collected for a sample of finchite from the
269 Pandora mine, and results are included in Table S7 (supporting information). The powder
270 diffractogram of finchite was also simulated from single crystal data for the Sulfur Springs Draw
271 sample and is compared with experimental powder diffraction data from Pandora finchite in
272 Supporting Information Figure S1. Calculated *d* values and intensities derived from the single
273 crystal structure are presented in Table S8.

274 ## IMPLICATIONS

275 The uranium deposits in the US Southwest were heavily mined during the Cold War and the
276 many tons of uranium ore that were recovered from this region fueled plutonium-production
277 reactors in Washington and South Carolina. Legacies of this activity include hundreds of inactive
278 mines and their associated tailings (Avasarala et al. 2017; Avasarala et al. 2020), more than 228
279 large underground nuclear waste storage tanks in Washington (Peterson et al. 2008; Stubbs et al.
280 2009; Christensen et al. 2004) and South Carolina (Evans 1992), and extensive subsurface
281 contamination at former nuclear weapon production sites. Modeling the environmental transport
282 of U, radionuclides, and heavy metals, such as Sr, requires a detailed understanding of the
283 minerals that form and limit their mobility.

284 ## ACKNOWLEDGEMENTS

285 The authors thank Ashley Shields and Andrew Miskowiec for helpful discussions and comments.
286 Reviewers Giuseppina Balassone and Jakub K. Plasil are also thanked for their constructive

comments, which improved the manuscript. This work was supported by the Department of Energy, Basic Energy Sciences, Heavy Elements Program under grant number DE-FG02-07ER15880. Analyses were conducted at the ND Energy Materials Characterization Facility at the University of Notre Dame.

REFERENCES

Armstrong, J.T., Quantitative Analysis of Silicates and Oxide Minerals: Comparison of Monte-Carlo, ZAF and Phi-Rho-Z procedures in Microbeam Analysis. D.E. Newbury, Editor. 1988, San Francisco Press Inc.: San Francisco, CA.

Avasarala, S., et al., Crystal chemistry of carnotite in abandoned mine wastes. Minerals, 2020. 10(10): p. 883.

Avasarala, S., et al., Reactive transport of U and V from abandoned uranium mine wastes. Environmental Science and Technology, 2017. 51(21): p. 12385–12393.

Barton, I.F., Barton, M.D., Thorson, J. Characteristics of Cu and U-V deposits in the Paradox Basin (Colorado Plateau) and associated alteration. Society of Economic Geologists, Inc. Guidebook Series, Volume 59. p. 73-102

Barton Jr., P.B., Synthesis and properties of carnotite and its alkali analogues. American Mineralogist: Journal of Earth and Planetary Materials, 1958. 43(9–10): p. 799–817.

Bruker, A., Saint and SADABS. Bruker AXS Inc., Madison, Wisconsin, USA, 2009.

Burciaga-Valencia, D., et al., Characterization of uranium minerals from Chihuahua using synchrotron radiation. Revista Mexicana de Física, 2010. 56(1): p. 75–81.

Burns, P.C., Ewing, R.C. and Hawthorne, F.C. The crystal chemistry of hexavalent uranium: polyhedron geometries, bond-valence parameters, and polymerization of polyhedra. Canadian Mineralogist, 1997. 35: p. 1551–1570.

Carter, W.D., Gualtieri, J.L., Geology and uranium-vanadium deposits of the La Sal Quadrangle, San Juan County, Utah and Montrose County, Colorado. 1958, USGS Report 508, 82 p.

Cejka, J., Infrared spectroscopy and thermal analysis of the uranyl minerals. Uranium: Mineralogy, Geochemistry and the Environment, 1999: p. 521–622.

Cesbron, F. and Morin, N. Curienite, A new mineral species. A study of the series francevillite-curienite. 1968, Laboratoire de Mineralogie-Cristallographie, Paris.

Christensen, J.N., et al., Identifying the sources of subsurface contamination at the Hanford Site in Washington using high-precision uranium isotopic measurements. Environmental Science and Technology, 2004. 38(12): p. 3330–3337.

Evans, A., et al., Uranium in the Savannah River Site environment. 1992, Westinghouse Savannah River Co., Aiken, SC, USA.

Finch, W.I., Geology of epigenetic uranium deposits in sandstone in the United States. 1967, USGS Professional Paper 538, 121 p.

Frye, J., et al., Late-Pleistocene Lake Lomax in western Texas, in Means of Correlation of Quaternary successions. 1968, University of Utah Press Salt Lake City. p. 519–534.

Glebov, V., Electronic structure and properties of uranyl compounds. Relation between bond length and bond strength in uranyl compounds. Koordinatsionnaya Khimiya, 1982. 8(7): p. 970–976.

Gunasekaran, S., G. Anbalagan, and S. Pandi, Raman and infrared spectra of carbonates of calcite structure. Journal of Raman Spectroscopy, 2006. 37(9): p. 892–899.

Hålenius, U., et al., New minerals and nomenclature modifications approved in 2017. Mineralogical Magazine, 2017. 81(5): p. 1279–1286.

Hall, S., et al., Calcrete uranium deposits in the Southern High Plains, USA. Ore Geology Reviews, 2019. 109: p. 50–78.

Jones, L.H., Systematics in the vibrational spectra of uranyl complexes. Spectrochimica Acta, 1958. 10(4): p. 395–403.

Kampf, A.R., et al., Pandoraite-Ba and Pandoraite-Ca, $Ba(V^{4+}_5V^{5+}_2)O_{16}\cdot 3H_2O$ and $Ca(V^{4+}_5V^{5+}_2)O_{16}\cdot 3H_2O$, two new vanadium oxide bronze minerals in solid solution from the Pandora Mine, La Sal Mining District, San Juan County, Colorado, USA. The Canadian Mineralogist, 2019. 57(2): p. 255-265.

Krivovichev, S.V., et al., Mineralogy and crystallography of uranium. Uranium: From Cradle to Grave. Mineralogical Association of Canada Short Courses, 2013. 43: p. 15–119.

Libowitzky, E., Correlation of O–H stretching frequencies and O–H···O hydrogen bond lengths in minerals. Monatshefte Für Chemie, 1999. 130(8): p. 1047–1059.

Peterson, R.E., et al., Uranium contamination in the subsurface beneath the 300 Area, Hanford Site, Washington. 2008, Pacific Northwest National Laboratory, Richland, WA, USA.

Piret, P., and M. Deliens, The Gladstone-Dale constant k (UO_3) for uranyl phosphates and arsenates. Canadian Mineralogist, 1989. 27: p. 533–534.

Plasil, J., Oxidation-hydration weathering of uraninite: the current state-of-knowledge. Journal of Geosciences, 2014. 59(2): p. 99–114.

Ranalli, A.J., Yager, D.B. Use of mineral/solution equilibrium calculations to assess the potential for carnotite precipitation from groundwater in the Texas Panhandle, USA. Applied Geochemistry, 2016. 73: p. 118-131

Sheldrick, G.M., Crystal structure refinement with SHELXL. Acta Crystallographica Section C: Structural Chemistry, 2015a. 71(1): p. 3–8.

———SHELXT–Integrated space-group and crystal-structure determination. Acta Crystallographica Section A: Foundations and Advances, 2015b. 71(1): p. 3–8.

Spano, T., Olds, T.A., Hall, S.M., and A.R. Kampf, Lowers, H. and Burns, P.C., Finchite, IMA 2017-052. Mineralogical Magazine, 2017a. p 81.

Spano, T.L., et al., Thermodynamic investigation of uranyl vanadate minerals: Implications for structural stability. American Mineralogist: Journal of Earth and Planetary Materials, 2017a. 102(6): p. 1149–1153.

Spano, T., Olds, T.A., Hall, S.M., and A.R. Kampf, Lowers, H. and Burns, P.C., Finchite, IMA 2017-052. Mineralogical Magazine, 2017b. p 81.

Stubbs, J.E., et al., Newly recognized hosts for uranium in the Hanford Site vadose zone. Geochimica et Cosmochimica Acta, 2009. 73(6): p. 1563–1576.

Tokunaga, T.K., et al., Aqueous uranium (VI) concentrations controlled by calcium uranyl vanadate precipitates. Environmental Science and Technology, 2012. 46(14): p. 7471–7477.

Van Gosen, B.S., and Hall, S.M., The discovery and character of Pleistocene calcrete uranium deposits in the Southern High Plains of west Texas, United States: U.S. Geological Survey Scientific Investigations Report 2017–5134, 2017, 27 p., https://doi.org/10.3133/sir20175134.Weeks, A.D., Mineralogy and geochemistry of vanadium in the Colorado Plateau. Journal of the Less Common Metals, 1961. 3(6): p. 443–450.

This is the peer-reviewed, final accepted version for American Mineralogist, published by the Mineralogical Society of America.
The published version is subject to change. Cite as Authors (Year) Title. American Mineralogist, in press.
DOI: https://doi.org/10.2138/am-2022-8365. http://www.minsocam.org/

Supporting Information

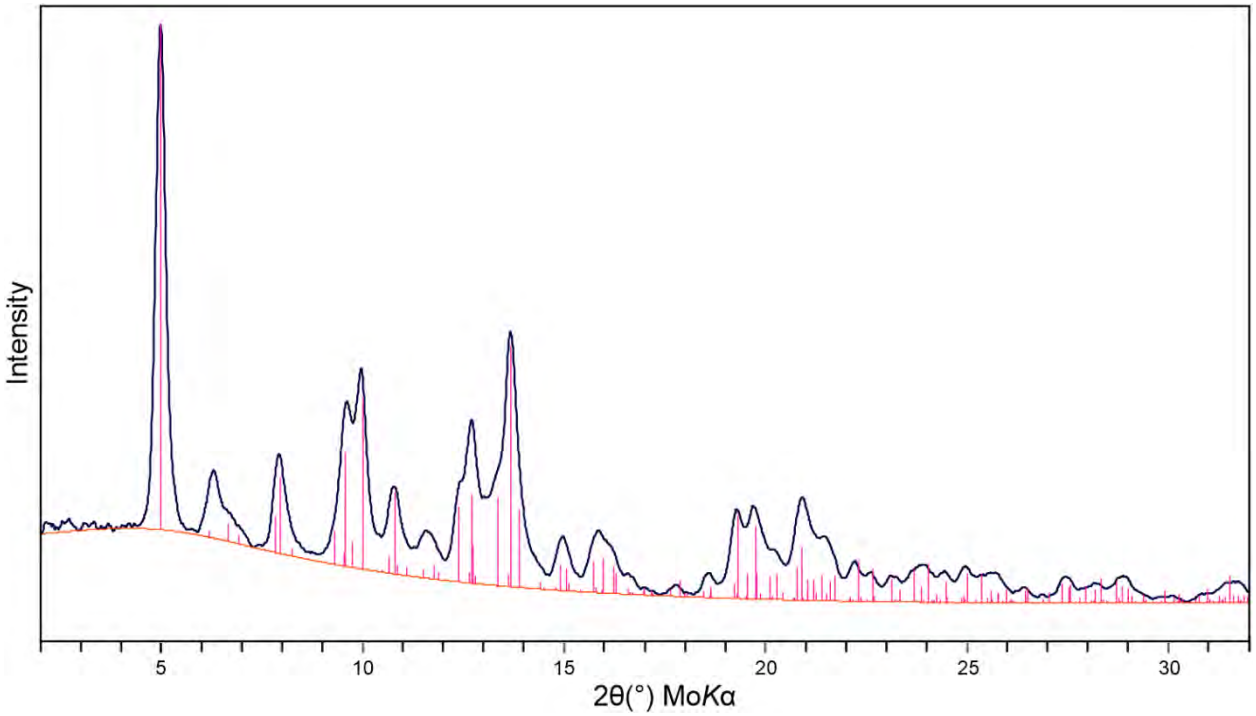

Figure S1. Simulated powder diffraction data for finchite from Sulfur Springs Draw (red) compared with experimental diffraction data collected for Pandora finchite (blue).

This is the peer-reviewed, final accepted version for American Mineralogist, published by the Mineralogical Society of America.
The published version is subject to change. Cite as Authors (Year) Title. American Mineralogist, in press.
DOI: https://doi.org/10.2138/am-2022-8365. http://www.minsocam.org/

Table 1. Chemical composition (in wt%) for finchite.

Constituent	Sulfur Springs Draw					Pandora mine			
	Mean (10 spots)	Range	Standard Dev.	Standard	Normalized	Mean (11 spots)	Range	Standard Dev.	Standard
K_2O	0.91	0.12-2.13	0.88	orthoclase	0.83	0.24	0.09-0.99	0.28	orthoclase
SrO	10.43	9.01-11.32	0.93	celestine	9.46	5.62	5.30-5.97	0.21	$SrTiO_3$
CaO	0.65	0.48-0.94	0.19	wollastonite	0.59	1.67	1.48-1.82	0.10	wollastonite
BaO						4.18	3.87-4.46	0.20	barite
MgO	0.16	0.05-0.44	0.13	olivine	0.15				
FeO	0.08	0.00-0.11	0.03	syn. fayalite	0.07				
Al_2O_3	0.19	0.00-0.31	0.08	anorthite	0.17				
V_2O_5	21.57	20.99-22.32	0.41	V_2O_5	19.57	19.74	19.14-20.28	0.38	V metal
UO_3	65.60	64.49-66.57	1.11	syn. UO_2	59.53	61.17	59.46-61.93	0.89	syn. UO_2
H_2O*	10.61				9.63	9.75			
Total	110.20				100.00	102.37			

Table 2. Data collection and structure refinement details for finchite.

Crystal Data	**Sulfur Springs Draw**	**Pandora mine**
Diffractometer	Bruker Apex II Quazar	Rigaku R-Axis Rapid II
X-ray radiation/power	Mo*K*α (λ = 0.71075 Å)	Mo*K*α (λ = 0.71075 Å)
Temperature	100(2) K	293(2) K
Structural Formula	$(Sr_{0.88}K_{0.17}Ca_{0.10})(UO_2)_2(VO_4)_2 \cdot 5H_2O$	$(Sr_{0.50}Ca_{0.28}Ba_{0.22})(UO_2)_2(VO_4)_2 \cdot 5H_2O$
Space group	*Pcan*	*Pcan*
Unit cell dimensions	a = 10.363(6) Å	a = 10.3898(16) Å
	b = 8.498(5) Å	b = 8.5326(14) Å
	c = 16.250(9) Å	c = 16.376(3) Å
V	1431.0(13) Å^3	1451.8(4) Å^3
Z	4	4
Density (for above formula)	4.352 g/cm^3	4.279 g/cm^3
Absorption coefficient	27.246 mm^{-1}	26.966 mm^{-1}
F(000)	1619	1612
Crystal size	14 × 10 × 3 μm	150 x 90 x 20 μm
θ range	2.51 to 24.99°	3.09 to 23.24°
Index ranges	$-12 \le h \le 12, -10 \le k \le 10, -19 \le l \le 19$	$-10 \le h \le 11, -9 \le k \le 8, -18 \le l \le 18$
Reflections collected/unique	13105/1259; R_{int} = 0.209	4561/997; R_{int} = 0.0793
Reflections with $F > 4\sigma F$	736	757
Completeness to θ_{max}	100%	95.3%
Refinement method	Full-matrix least-squares on F^2	Full-matrix least-squares on F^2
Restraints/parameters	196/102	0/101
GoF (ref/all)	1.022/0.948	1.094/1.094
Final R indices [$F > 4\sigma(F)$]	R_1 = 0.0555, wR_2 = 0.1240	R_1 = 0.0600, wR_2 = 0.1576
R indices (all data)	R_1 = 0.1172, wR_2 = 0.1490	R_1 = 0.0796, wR_2 = 0.1711
Largest diff. peak/hole	+3.28/–2.28 e·A^{-3}	+2.58/–1.47 e·A^{-3}

*$R_{int} = \Sigma|F_o^2 - F_o^2(\text{mean})|/\Sigma[F_o^2]$. GoF = $S = \{\Sigma[w(F_o^2 - F_c^2)^2]/(n-p)\}^{1/2}$. $R_1 = \Sigma||F_o| - |F_c||/\Sigma|F_o|$. $wR_2 = \{\Sigma[w(F_o^2 - F_c^2)^2]/\Sigma[w(F_o^2)^2]\}^{1/2}$; $w = 1/[\sigma^2(F_o^2) + (aP)^2 + bP]$ where P is $[2F_c^2 + \text{Max}(F_o^2, 0)]/3$, a is 0.0538, and b is 75.381 from Sulfur Springs Draw. From the Pandora mine, a is 0.0725, and b is 79.984.